Quantifying the response of piled structures from displacements induced by pile installation in soft clay

Canadian Geotechnical Journal

OPEN ACCESS | Research Article

Quantifying the response of piled structures from displacements induced by pile installation in soft clay

Jonatan Isaksson[a,b], **Mats Karlsson**[b], **and Jelke Dijkstra**[b]

[a]NCC Sverige AB, Department of Research and Innovation, SE-17080 Solna, Sweden; [b]Chalmers University of Technology, Division of Geology and Geotechnics, SE-41296 Gothenburg, Sweden

Corresponding author: **Jonatan Isaksson** (email: jonatan.isaksson@chalmers.se)

Abstract

The impact of pile installation in soft soils on its surroundings has been numerically investigated with a focus on the response of an existing piled structure. The originality is the parameterised 3D finite element analyses of far-field soil–structure interaction scenarios, i.e., interactions that are largely driven by mass-displacements. A main finding is that the geometry, which includes the number and length of newly installed and existing piles, the distance between the two pile groups, and also the distance to stiff boundaries in the system (in the field and in the numerical analysis), governs the problem to a large extent. Therefore, to simplify the analysis of such complex cases, modification factors for the displacements in greenfield conditions are proposed, to calculate the displacement and structural response of the existing structure. The proposed non-dimensional factors are a function of the length of the newly installed and existing piles and the distance between the two pile groups. No unique solution exists; hence, a series of charts have been compiled to provide a first assessment of the impact of an existing piled structure on the induced displacements from the installation of a nearby group of displacement piles in soft soil.

Key words: clay, soil-structure interaction, pile installation, displacements, building response

Résumé

L’impact de l’installation des pieux dans les sols mous sur ses environs a été numériquement investigé avec un accent sur la réponse d’une structure à pieux existante. L’originalité est les analyses paramétrées par éléments finis en 3D des interactions sol-structure-à grande distance scénarios, c’est-à-dire des interactions qui sont largement déterminées par des déplacements de masse. Une des principales conclusions est que la géométrie, qui inclut le nombre et la longueur des nouveaux installés et existants pieux, la distance entre les deux groupes de pieux et aussi la distance aux limites rigides dans le système (sur le terrain et dans l’analyse numérique), régissent le problème dans une large étendue. Par conséquent, pour simplifier l’analyse de ces cas complexes, des facteurs de modification pour les déplacements dans en conditions de terrain vierge sont proposées, afin de calculer le déplacement. et la réponse structurelle de la structure existante. Les facteurs non dimensionnels proposés sont une fonction de la longueur des pieux nouvellement installés et existants et de la distance entre les deux groupes de pieux. Aucune solution unique n’existe, c’est pourquoi une série de graphiques ont été compilées pour fournir une première évaluation de l’impact d’une structure à pieux existante sur les déplacements induits par l’installation d’un groupe de déplacement à proximité pieux dans un sol mou.

Mots-clés : argile, interaction sol-structure, installation de pieux, déplacements, bâtiment reponses

1. Introduction

Geotechnical design in an urban setting involves the mitigation of damage to existing structures (Burland 1997). Xu and Poulos (2001) discuss potential situations in which externally induced displacements in the soil from nearby construction activities can lead to additional forces and stress in existing structures on shallow or deep foundations. One source of induced soil displacements is the installation of displacement piles in fine-grained soils, such as clay. Pile installation generates vertical and horizontal displacements in the soil at a radial distance exceeding the installed pile length (e.g., Hagerty and Peck 1971; Bozozuk et al. 1978; Dugan and Freed 1984; Edstam and Kullingsjö 2010). The displaced soil from pile installation is also called mass-displacement, in case the response of the clay is largely undrained without volume change. Dugan and Freed (1984) reported a considerable difference between the displacements from pile installation in greenfield (GF) conditions, i.e., homogeneous soil, level surface, without existing structures, and the displacements of an existing structure embedded at the same location. The emerging displacement of the existing structure, and its foundation, is a result of the soil–structure interaction (SSI), involving three parts:

- the induced displacements of the soil from the pile installation process at the *source*;
- the relative stiffness between the structure and the soil at the *receiver*;
- the geometrical constraints and properties of the soil in between the source and receiver; the *medium*.

The modification factors approach originally developed and improved for assessing the impact of volume loss from tunnelling on existing foundations (e.g., Potts and Addenbrooke 1997; Franzius et al. 2006; Mair 2013; Franza et al. 2017, 2021), has been successfully used to quantify the impact of SSI in other geotechnical engineering problems, where externally induced soil displacements interact with an existing structure, e.g., excavations (e.g., Korff 2012; Goh and Mair 2014; Zheng et al. 2023) or regional subsidence (e.g., Deck and Singh 2012; Basmaji et al. 2019; Franza et al. 2020). In the modification factors approach the GF displacements are scaled with a factor accounting for the effect of the relative stiffness, distance and foundation layout of the affected structure. The magnitude of the factors are derived based on numerical analyses using the finite element method (FEM). The modification factors approach have not yet been developed for cases where the induced displacements acting on existing structures stem from nearby installation of displacement piles in clay.

The impact of pile installation on the clay surrounding the pile has been extensively studied in field (e.g., Karlsrud and Haugen 1985; Lehane and Jardine 1994; Hunt et al. 2002) and laboratory tests (e.g., Lehane and Gill 2004; Ni et al. 2010), as well as by numerical modelling (e.g., Sheil et al. 2015; Abu-Farsakh et al. 2015; Monforte et al. 2021). These studies, however, mainly focus on the changes in effective stress and other state variables and the displacements in the near-field. The far-field effects, i.e., at a distance beyond notable stress change, are not as commonly investigated and are mainly present as a translation of a soil mass, as the change in state of the soil (from deformations) are small (Bozozuk et al. 1978; Edstam and Kullingsjö 2010). Yet, many unresolved issues in geotechnical engineering projects in an urban setting arise between new and existing structures that interact in the far-field.

The short-term (instantaneous) soil displacements due to installation of displacement piles in soft soils can be directly related to the installed pile volume, given the undrained loading conditions that emerge from the low hydraulic conductivity of the clay and the high loading rate during pile installation (Randolph et al. 1979). The emerging drainage conditions during pile installation can be estimated by the normalised penetration velocity as $V = \frac{vd}{c_v}$, where v is the installation velocity, d is the diameter of the pile, and c_v is the vertical consolidation coefficient where a normalised penetration velocity higher than 20 are indicating an undrained system response (Lehane et al. 2009). The short-term constant volume displacements are experimentally supported by Ni et al. (2010) in a laboratory and by Edstam and Kullingsjö (2010) in the field. In the long-term, the consolidation-driven movement, following the dissipation of excess pore pressures from driving, has been found to be in the reversed direction due to consolidation compared to the installation movement (Dugan and Freed 1984; Pestana et al. 2002). Thus, the largest displacement is found in the short-term situation. The shallow strain path method (SSPM) (Sagaseta et al. 1997) has been shown to capture the measured displacements from installing a single pile when benchmarked against both a field and laboratory test (Sagaseta and Whittle 2001; Ni et al. 2010; Zhou et al. 2017). Additionally, SSPM can also be used to predict the mass-displacements from multiple piles by superposition of the solution for a single pile (Sagaseta and Whittle 2001; Edstam and Kullingsjö 2010).

SSPM, however, does not directly account for the influence of the interaction between existing structures and surrounding soil on the distribution of displacements. Therefore, SSPM needs to be extended for use cases with an existing structure by introducing modification factors.

The current work aims to expand the use of the modification factors approach towards displacements from pile installation in soft soils. The focus is on quantifying the impact of an existing structure on the change in displacements in the clay surrounding its foundation. Therefore, a systematic parametric study has been performed to quantify the influence of distance, new and existing pile lengths, relative foundation–soil stiffness and spacing of existing piles on the deformation behaviour of the existing deep foundation. The results will be compiled in a series of charts for modification factors that can be used in (complex) engineering settings, where the magnitude of the predicted displacements without structure might be either obtained empirically, based on a simplified prediction method (e.g., Sagaseta et al. 1997) or evaluated from monitoring data.

2. Methodology

2.1. Model concept

The numerical model for the parametric study on the impact of soil–structure interaction between a volume change from pile installation at the source and the displacements around an existing deep foundation is developed within the FEM using PLAXIS 3D (Brinkgreve et al. 2023). The problem requires a three-dimensional (3D) finite element (FE) model to incorporate the geometrical effects of the displacements adjacent to multiple piles. Hence, a simplified SSI has been created to reduce the model complexity and computational demand, given the focus is on establishing a relation between the GF displacements and the response of existing structural elements at a distance from the source. Three main simplifications are made in, respectively, the *source*, the *receiver*, and the *medium*.

- The *source* of the mass-displacement from pile installation is modelled using a horizontal cavity expansion for the complete pile group (Edstam and Kullingsjö 2010). Numerical cavity expansion substantially simplifies analysis com-

pared to modelling the actual vertical penetration mechanism, which requires special numerical techniques to handle large deformations (e.g., Wang et al. 2015). In the case considered herein this simplification is permissible, as the distance between the source and receiver is sufficiently large (Isaksson 2022).
- The existing structure at the *receiver* side is modelled using embedded beams (EBs) (Sadek and Shahrour 2004) for the piles and plate elements for the foundation slab. Therefore, the number of degrees of freedom in the numerical model is greatly reduced when compared to using solid volume elements (Sheil and McCabe 2012).
- The soil in the *medium* is modelled as a linear elastic (LE) solid with an equivalent stiffness and Poisson's ratio that reflect an undrained soil response. The LE model provides a conservative estimate for the magnitude of the modification factors, whilst sacrificing some accuracy near the source of the generated displacements, whereas at the larger distances with only small (shear) deformations, the response is captured well.

Combined the three simplifications enable the study of modification factors for a large number of cases whilst incorporating, in a simplified manner, a pile group on both the source and receiver ends. The modelled undrained conditions (constant volume) are valid in the short-term situation for a pile installed in a soft soil, before the consolidation of the excess pore pressures results in a volume change of the soil in the vicinity of the driven piles. Due to consolidation, the constant volume conditions are no longer valid, which for soft soil leads to reduced soil displacements. Lower displacements can, in a first assessment be assumed to reduce the risk of damage to an existing structure.

Given the model simplifications, the results from this study are applicable when the distance of the existing foundation is beyond ≈10 pile diameters (Isaksson 2022). For common pile diameters used in Sweden, the distance is less than the width of a street but larger than practical pile spacings. In the far field, the cumulative effect of the displacements from multiple piles will be the more critical design situation.

2.2. Modelling displacements from pile group

The installation method used for the pile group in the 3D FE model is a further development of the approach suggested in Edstam and Kullingsjö (2010). The suggested approach shows comparable performance against SSPM and good agreement with measured displacements in GF conditions for a field test.

Numerically, the installation of a pile (group) is modelled by the expansion of a predefined soil volume, extending from the surface down to a depth corresponding to the pile length. The volume is expanded in the two horizontal directions of the domain where the added volume represents the installed pile volume. A schematic illustration of the modelling framework is presented in Fig. 1. The initial area A_i of the soil is expanded to a new area A_{exp} and the difference Ω corresponds to the installed pile volume per meter of the installed pile or pile group. The constant volume behaviour of natural clay during the installation process is captured with an LE total stress formulation using an undrained stiffness combined with a Poisson's ratio $\nu = 0.499$.

Fig. 1. Schematic illustration of the expanded cross-section over the length of the pile.

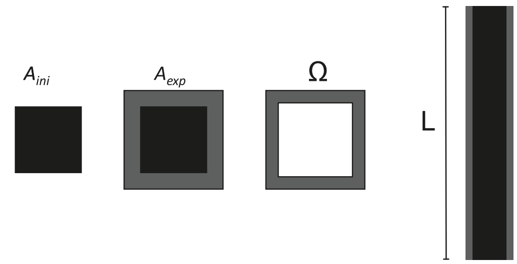

2.3. Modelling existing piled structure

The existing deep foundation is modelled in a simplified manner using structural elements. The superstructure of the existing building is included using a plate representing a simple slab resting on top of the soil. The connection between the plate and the soil is modelled as fully bonded. Preliminary investigations were performed where an interface element was used for the connection between the soil and the slab. A stiffness reduction of 50% did not induce any major changes to the observed behaviour with respect to the restraint caused by the existing foundation. The piles below the existing structure are modelled with EBs (Sadek and Shahrour 2004). EB is more efficient than modelling piles with volume elements, which enables the systematic study of more scenarios with a large number of piles (Sheil and McCabe 2012). A previous version of EB than currently implemented in PLAXIS (Tschuchnigg and Schweiger 2015) has been used to model lateral loading on piles in soft soils (Dao 2011). When combining the EB with aand LE soil, PLAXIS automatically sets the interface stiffness and strength, which disables any user selection of interface behaviour. The most recent implementation is not fully verified for the case of mass-displacement induced lateral pile deflections. A numerical verification was, therefore, conducted to compare the response of an EB pile and a volume pile (VP) in a LE model.

The numerical 3D model for comparison of the VP and the embedded pile is presented in Fig. 2. The domain of the model is 4 m wide and 60 m long and has a depth of 35 m. Approximately 270 000 10-noded tetrahedrons are used to mesh the domain with a refined zone starting 2.5 m before until 2.5 m after the existing pile. At the receiver end an existing square concrete pile ($w = 275$ mm) with a stiffness E of 30 GPa is pre-installed in an LE soil with a Poisson's ratio of 0.499 and a shear modulus G of 3 MPa.

The existing pile is placed 15 m from the source of the soil displacements and is 30 m long. The pile displacement is simulated at the left side (source) of the domain by a horizontal expansion of a volume cluster that is 1 m wide and 30 m deep. Finally, two vertical cross sections, $L1$ and $L2$, are defined 0.5 m in the y-direction and ± 0.5 m in the x-direction from the pile, to monitor the displacement in the soil close to the pile.

Fig. 2. Numerical model to compare the response of a volume pile and an embedded beam.

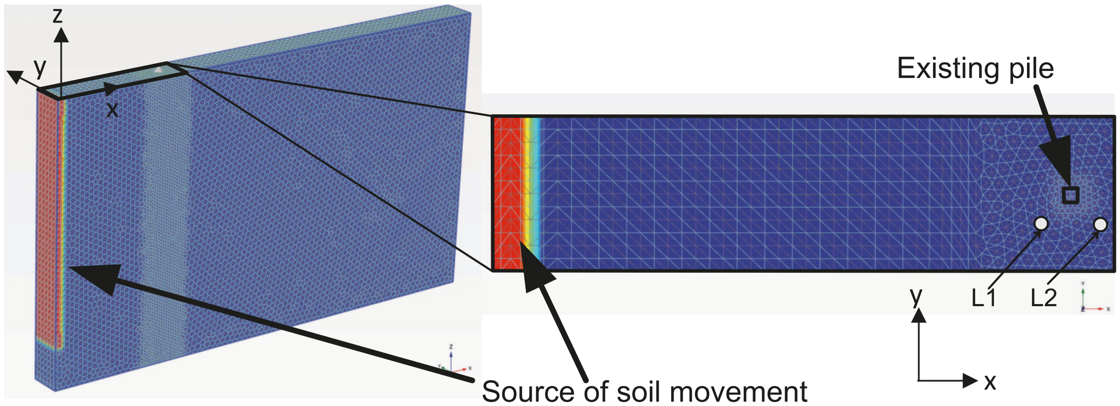

Fig. 3. Deflection of embedded beam (EB) and volume pile (VP) compared to greenfield displacements (GF) at the location of the existing structure: (*a*) free pile; (*b*) laterally fixed pile.

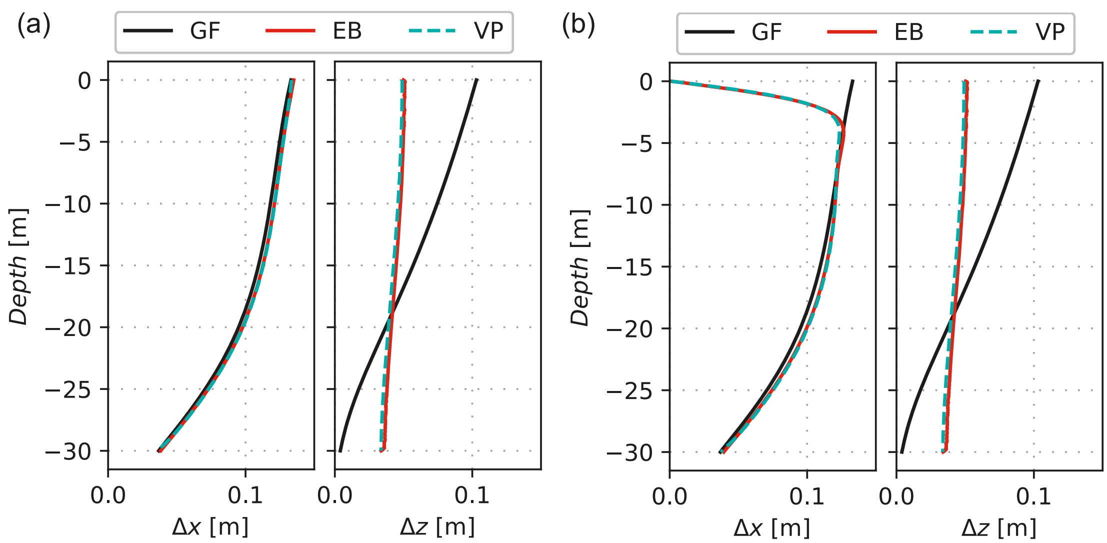

Figure 3 shows that the EB predicts, for the numerical modelling approach considered, similar deflection behaviour as the VP when using a fixed or a free moving pile head as boundary condition. Furthermore, the displacements of the soil surrounding the pile in the case of a laterally fixed pile head are presented in Fig. 4. Also in this case, the soil displacements are largely similar when comparing the response from the VP and the EB.

The numerical verification shows that the use of EB elements is warranted for modelling the existing foundation in the problem at hand. Consequently, in the following only EB will be used to model the piles below the existing structure.

3. Response of an existing piled structure

3.1. Parameterised model

A parameterised numerical model was created for the systematic investigation of the impact of an existing piled structure on the displacement field surrounding it. A schematic illustration is presented in Fig. 5. The pile installation is modelled at the centre of the domain, along the symmetry plane, by prescribing horizontal strains corresponding to the added pile area Ω along the full length of the installed pile L_i. The existing piled structure is placed at a distance D from the installed pile and consists of several EBs with length L_{ex}. The EBs are placed in a square grid, with a centre-to-centre spacing ctc connected to a horizontal plate. Side b is directed along the symmetry plane, whilst side w is in the perpendicular direction. Horizontal displacements in the normal direction are fixed on the vertical boundaries for the soil and structural elements. A typical mesh of the parameterised model is presented in Fig. 6 and consists of ca. 274 000 10-noded tetrahedrons. The unstructured mesh is refined in a larger section containing both the existing piled structure and the newly installed pile group. Additional refinements are defined around the existing piled structure and the newly installed pile group. The parameterised model shown in Fig. 6 utilises half symmetry and

Fig. 4. Soil displacements in the vicinity of the fixed pile using the embedded beam (EB) and a volume pile (VP) compared to greenfield displacements (GF) at the same location: (*a*) soil displacement: L1; (*b*) soil displacement: L2.

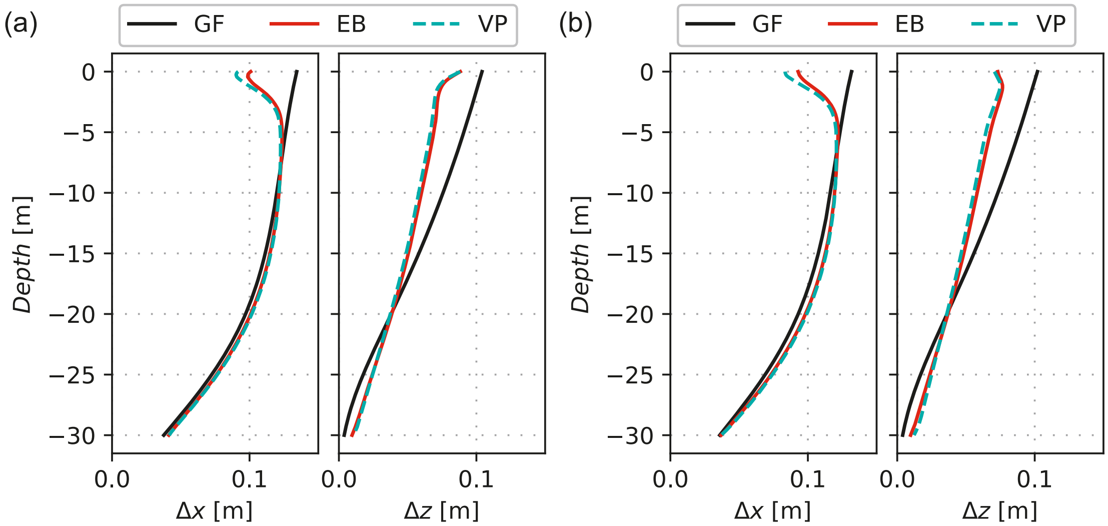

Fig. 5. Schematic illustration of the numerical model.

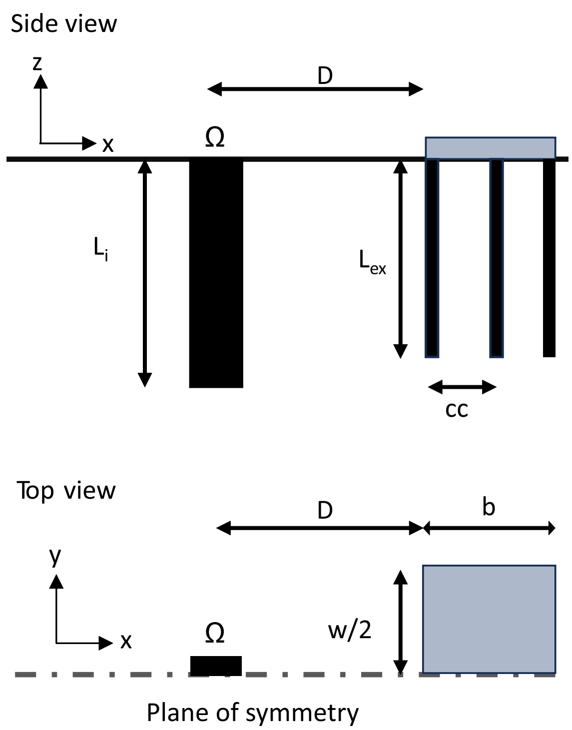

the rectangular domain has sides $S_1 = S$, $S_2 = 2S$, and a soil depth d.

The soil is modelled with a LE model using model parameters that capture the undrained soil response of a typical natural soft clay from Gothenburg, Sweden, see Table 1. The slightly overconsolidated clay has a linearly increasing stiffness with depth and the Poisson's ratio is chosen to obtain near constant volume response. Furthermore, an equivalent $K_{0T} = 0.85$ for total stress is derived from the measured $K_0 = 0.6$ for Gothenburg conditions. The basic model parameters for the structural elements are specified in Tables 2 and 3 for the EB and plate, respectively. These tabulated model parameters will be used in the following simulations unless otherwise specified. The connection between the plate and the EB is modelled as a pinned support.

3.2. Greenfield displacements

Prior to investigating the impact of the existing foundation, the behaviours of the GF soil displacements from the installation of the pile group as predicted by SSPM and FEM are compared. Sagaseta and Whittle (2001) show that SSPM produces a non-dimensional relationship for the GF displacements δ_{GF} in the radial r and vertical z directions as a function of the pile area Ω and installed pile length L_i: $\frac{\delta_{GF}\pi L_i}{\Omega} = f\left(\frac{r}{L_i}, \frac{z}{L_i}\right)$. This unique relation is valid for an infinite half-space. A stiff bottom at a finite depth, however, will alter the solution, thus introducing an additional dependency term which is $\left(\frac{d}{L_i}\right)$. Additionally, a dependency has been found on the extent of the soil deposit in the horizontal direction $(\frac{S}{L})$. The influence of the horizontal extent of the domain can either reflect a soft soil deposit contained by, for example, rock or the boundary of a numerical or experimental model. As such, a new dimensionless relation where the influence of a soil deposit with finite dimensions has been included can now be formulated as: $\frac{\delta_{GF}\pi L}{\Omega} = f\left(\frac{r}{L_i}, \frac{z}{L_i}, \frac{d}{L_i}, \frac{S}{L_i}\right)$.

The non-dimensional displacements are presented in Fig. 7. Figure 7*a* shows the results from five simulations with varying Ω and L_i according to the values reported in Table 4. The results show that the relation $\frac{\delta_{GF}\pi L_i}{\Omega} = f\left(\frac{r}{L_i}, \frac{z}{L_i}\right)$ proposed by Sagaseta and Whittle (2001) holds for the numerical cavity expansion method used for the installation method for the pile group. The influence of d/L_i is shown in Fig. 7*b*. The arrows represent the order of the datasets as specified in the textbox; i.e., the reduction in the d/L_i ratio leads to lower horizontal and higher vertical displacements at a specific loca-

Fig. 6. Full numerical model and detail showing the installed pile and existing foundation.

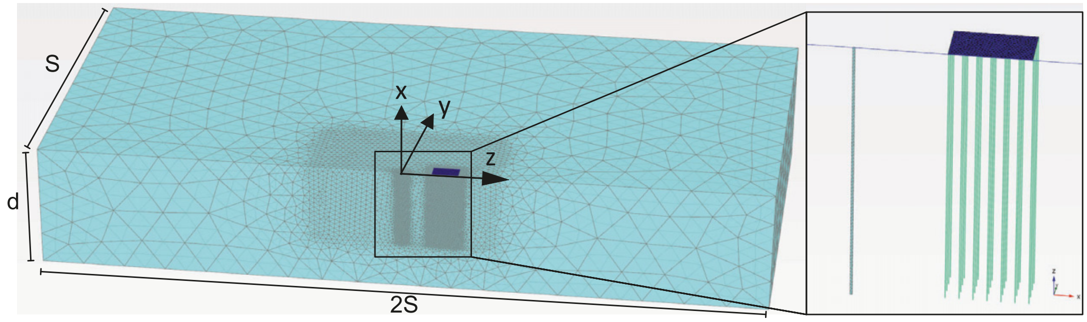

Table 1. Soil properties.

Material type	Drainage type	γ (kNm^{-3})	ν (−)	E_u (kPa)	$E_{u,\,\mathrm{inc}}$ (kPam^{-1})	K_{0T} (−)
Linear elastic	Undrained C	16	0.499	5625	506	0.85

Table 2. Embedded beam properties.

Material type	γ (kNm^{-3})	A (m^2)	E (GPa)	EA (kN)
Linear elastic	8	0.07563	30	2.269×10^6

tion. Figure 7*c* shows the strong influence of the horizontal extent of the soil deposit in which the pile is installed. The arrows represent the order of the datasets as specified in the textbox; i.e., the increase in the S/L_i ratio leads to vertical and horizontal displacements at a specific location. The radial displacements are approaching zero at the domain edge, which lead to larger vertical displacements from the constant volume assumption. In summary, the SSPM and FEM predictions of the GF displacements, although not identical due to the boundary effects, predict comparable order of magnitude and influence of the dimensionless group, accounting for relative location.

3.3. Influence of an existing piled structure

As an initial step, the displacement field of a reference configuration for the existing structure and its foundation were computed to give insight into the displacement behaviour from nearby pile installation. The details of this configuration (Fig. 5) are specified in Table 5.

Figure 8 shows the computed displacements with (F) and without (GF) existing structure in the radial and vertical direction along the symmetry plane. The impact of the existing structure, denoted *F*, on the results is plotted as the change in displacements relative to the GF displacements as $(\delta_F - \delta_{GF})/\delta_{GF}$. Figures 8*c* and 8*d* show that the distribution of soil displacements is significantly impacted by the presence of an existing foundation (indicated by the grey frame superimposed on the contour plot). The radial displacements are lower in the front and enclosed part of the foundation compared to the GF situation. In contrast, the displacements are larger than the GF displacements at a large distance towards depth and behind the foundation. The vertical component of the displacements is strongly influenced by the pile foundation, where the soil enclosed by the foundation experiences reduced displacement magnitudes. The exception is that the vertical displacements near the lower (resisting) part of the pile move upwards relative to the GF displacements.

The displacements of the slab and edge piles in the pile row closest to the symmetry boundary of the structure are presented in Fig. 9. The displacements are scaled with a factor of 20 000. Figure 9*a* shows that the vertical displacement in the front pile is smaller for the upper part, in contrast to the lower part, when compared to the GF situation. The vertical displacement is upwards for the pile while being downwards in the GF situation. The horizontal displacements are very similar for most of the lower part of the pile. However, in the upper part of the pile, see Fig. 9*b*, the GF displacements and deflection of the foundation are different in the horizontal direction. This is because the foundation slab approximately displaces as a rigid body in its stiff horizontal direction. Therefore, the front pile is held back and the back pile is pushed forward relative to the displacement of the lower part of the pile. The magnitude of the displacements in the centre location of the slab are nearly identical for both the foundation and the GF situation.

4. Parametric study on restraint effects

The detailed investigation is used to establish a group of response parameters (see Table 6) to quantify the response of the existing structure for subsequent parametric study of different foundation configurations as depicted in Fig. 5. The response parameters at the receiver are derived based on the displacements δ and deflection Δ for the slab and the pile, as elaborated in Figs. 10*a* and 10*b*. The vertical relative restraint $r_{z,\,F}$ and horizontal relative restraint $r_{x,\,F}$ quantify to what extent the displacement of the existing foundation deviates from the GF displacement at the same location. The mobilisation of axial strain in the pile ε_a is related to the axial load in the pile N as $\varepsilon_a = \frac{N}{A}$. The curvature κ can be directly related to the moment in the structural member by $\kappa = \frac{M}{\mathrm{EI}}$. As shown in Fig. 7*a*, no inflexion points are present in the

Table 3. Plate properties.

Material type	γ (kNm^{-3})	h (m)	ν (–)	E (GPa)	D (kN m^2 m^{-1})	EA (kN)
Linear elastic	24	0.3	0	30	8.1×10^5	9×10^6

Fig. 7. Non-dimensional surface displacements due to pile installation; $\frac{\delta_{GF}\pi L_i}{\Omega} = f\left(\frac{r}{L_i}, \frac{z}{L_i}, \frac{d}{L_i}, \frac{S}{L_i}\right)$: (*a*) $\frac{\delta_{GF}\pi L_i}{\Omega}$ when $d/L_i = 2.5$ and $S/L_i = 5$; (*b*) influence of d/L_i; (*c*) influence of S/L_i. SSPM, shallow strain path method; FEM, finite element method.

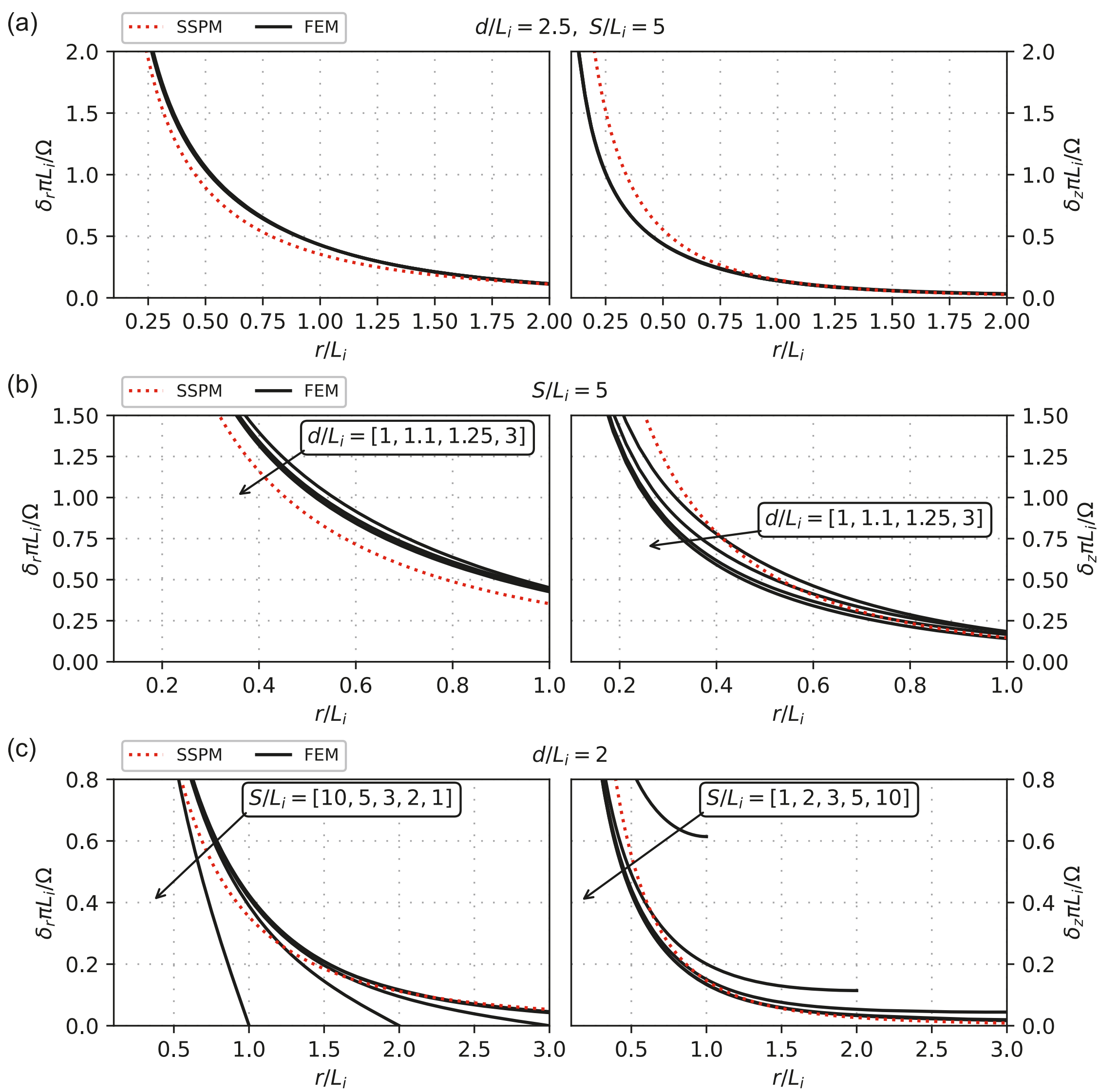

Table 4. Finite element simulations for investigating the non-dimensional group: $\frac{\delta_{GF}\pi L_i}{\Omega} = f\left(\frac{r}{L_i}, \frac{z}{L_i}\right)$.

Run	1	2	3	4	5
A_{ini} (m^2)	0.25	0.25	0.25	0.25	1
L_i (m)	40	60	80	40	40
ε_h (%)	15	15	15	30	15
Ω (m^2)	0.0756	0.0756	0.0756	0.15	0.30

distribution of vertical displacements for the slab, thus the deflection ratio of the slab DR is defined over the full foundation width. For slender piles, buckling is a failure mode that needs to be considered. The deflection ratio over a buckling length DR_{pile} should be quantified, to estimate the axial capacity reduction due to the bent shape of the deformed pile. The buckling length of the pile L_c is directly proportional to the stiffness of the pile and lateral support stiffness k of the

Table 5. Geometrical configuration for existing foundation in illustrative case (see Fig. 5).

L_i (m)	Ω (m^2)	D (m)	L_{ex} (m)	ctc$_x$ (m)	ctc$_y$ (m)	b (m)	w (m)
60	0.0756	20	60	3	3	18	21

Fig. 8. Pile installation induced displacements in greenfield conditions (GF) and the relative change of horizontal displacement due to an existing piled structure (F). The existing piled structure is indicated by a grey box: (*a*) horizontal GF; (*b*) vertical GF; (*c*) horizontal influence of foundation; (*d*) vertical influence of foundation.

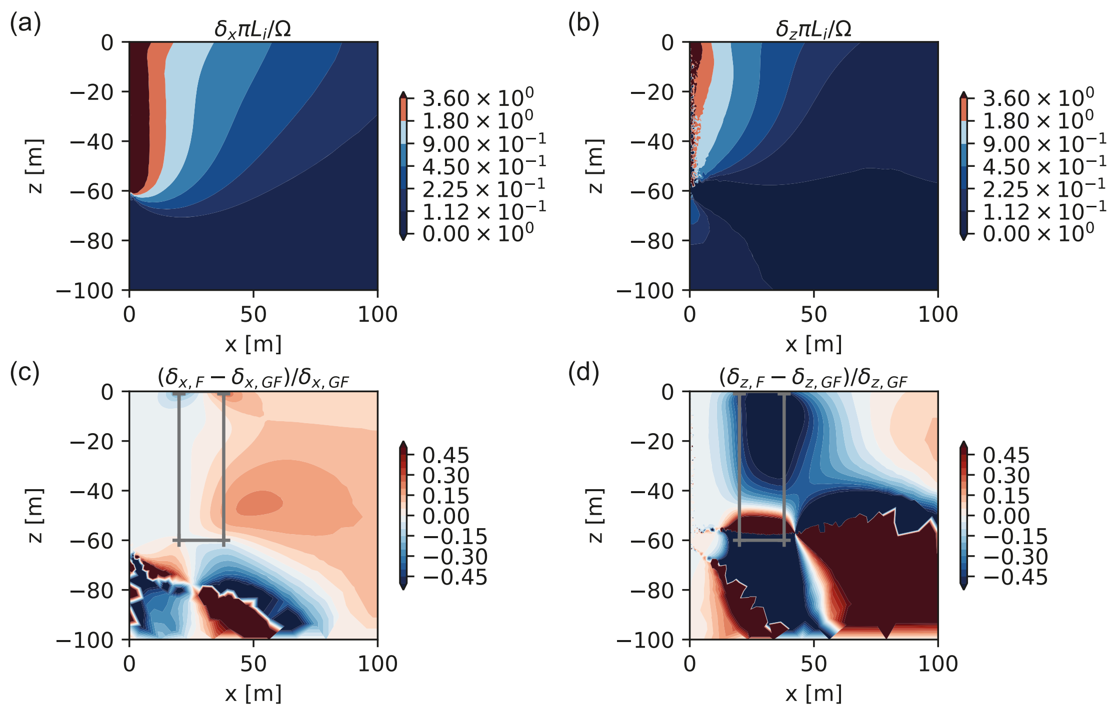

Fig. 9. Deflections of existing structure from nearby pile installation: (*a*) complete foundation; (*b*) close-up of slab–pile connection.

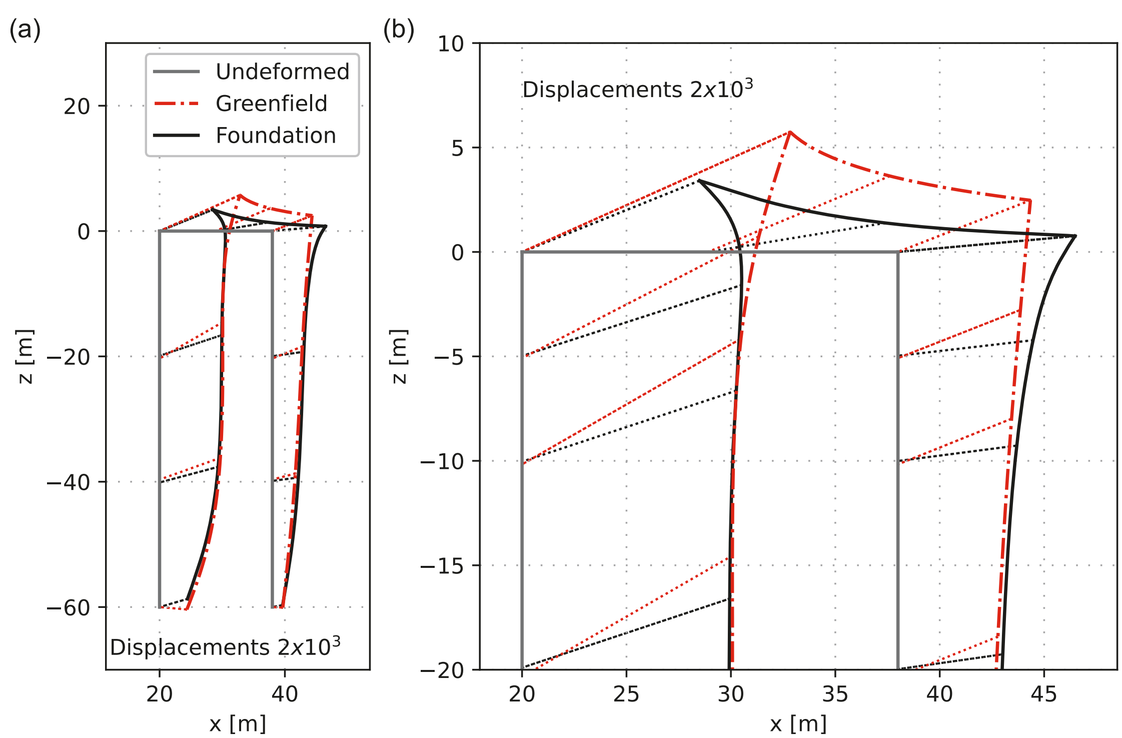

Table 6. Response parameters.

Symbol (unit)	Definition	Name
$r_{z,\,F}$ (−)	$\frac{\delta_{z,GF}-\delta_{z,F}}{\delta_{z,GF}}$	Vertical relative restraint
$r_{x,\,F}$ (−)	$\frac{\delta_{x,GF}-\delta_{x,F}}{\delta_{x,GF}}$	Horizontal relative restraint
DR (−)	Δ_z/b	Deflection ratio over foundation width
$\mathrm{DR_{pile}}$ (−)	$\Delta_{x,\,c}/L_c$	Deflection ratio over buckling length
Tilt (−)	$\frac{\delta_{start}-\delta_{end}}{b}$	Tilt
κ (m^{-1})	$1/R$ of a circle connecting three neighbouring points in distribution of δ	Curvature of slab/pile
ε_a (%)		Axial strain in pile

Fig. 10. Definition of normalised response parameters for the parametric study. (*a*) Surface; (*b*) depth.

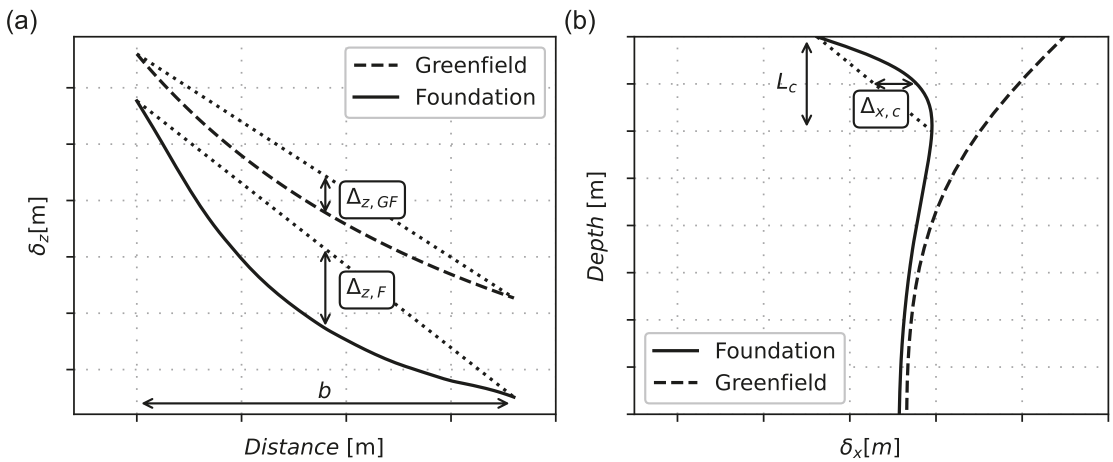

Table 7. Details of the parametric study on the relative pile length and relative distance between the existing structure and newly installed group.

L_i (m)	D (m)	L_{ex} (m)
40, 60, 80	10, 20, 30, 40, 50, 60, 70, 80	40, 60, 80

soil, i.e., $L_c = \pi(\mathrm{EI}/k)^{1/4}$ (e.g., Poulos and Davis 1980). In this work k is empirically linked to the undrained stiffness E_{soil} using two correlations commonly used in Gothenburg, i.e., $k = 80c_u$ in which $c_u = E_{soil}/375$. The parametric study is divided into two parts: L_i, L_{ex}, and D are investigated first, prior to studying the influence of ctc, foundation area, E_{soil}, E_{pile}, and E_{slab}.

4.1. Distance from source and pile length

The influence of relative distance and relative pile length, between the installed pile (group) and existing structure, are studied by varying D, L_i, and L_{ex}. All other model parameters and properties are kept constant, as specified in Tables 1, 2, and 3. The study was conducted by computing the results for all possible configurations shown in Table 7. The responses of the foundation slab are presented as contours in Fig. 11. The horizontal axis in the plot represents the relative distance between the installed piles (source) and existing structure (receiver) L_i/D and the vertical axis represents the relation between the pile length in the existing L_{ex} and newly installed L_i foundations $(L_i - L_{ex})/L_i$. This layout was inspired by Dias and Bezuijen (2015), who studied displacements of existing deep foundations due to tunnelling. The mean horizontal and vertical restraints of the slab are presented in Figs. 11*b* and 11*a* and are based on the sum of restraints along the width of the slab. The horizontal restraint shows that the displacement of the slab is very close to the mean GF displacements on the surface along the location of the slab. In contrast, the vertical restraints are above 0 for all foundation configurations and increase with an increased L_i/D and $(L_i - L_{ex})/L_i$.

The influence of the piled structure on the deflection ratio and tilt of the slab is shown in Fig. 12. For these two response parameters, the results for the individual L_i had to be separated, indicating that the response is not fully normalised by L_i/D and $(L_i - L_{ex})/L_i$. The $\mathrm{DR_F}/\mathrm{DR_{GF}}$ increases in regions with a higher $r_{z,\,F}$ (Fig. 11*a*) and decreases in regions with very low $r_{z,\,F}$. The tilt in most configurations, decreased with an existing structure present, but shows an increase for L_i of 60 and 80 m and $L/D \approx 0.5$ and $(L_i - L_{ex})/L_i$.

The front pile closest to the symmetry axis is chosen to study the response for the existing piles, as the middle edge piles are most representative for the system response. Detailed analyses should be performed in situations where piles in other locations of the group, especially the corner piles, are of importance. The results from the analyses are presented in Fig. 13. The vertical relative restraint $r_{z,\,F}$, see Fig. 13*a*, increases with the distance from the installed pile group and

Fig. 11. Influence of geometry on the displacements of the slab of an existing foundation (F) relative to the greenfield (GF) displacements from pile installation. (*a*) Relative vertical restraint ($r_{z,F}$), (*b*) relative horizontal restraint ($r_{x,F}$).

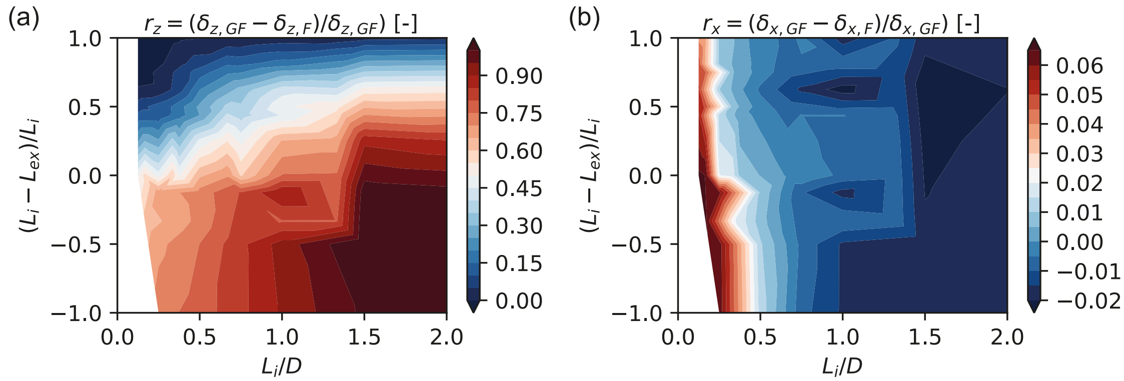

Fig. 12. Influence of geometry on the tilt and deflection ratio of the slab of an existing foundation (F) relative to the greenfield (GF) situation: (*a*) $Tilt_F/Tilt_{GF}$ (−), L_i = 40 m; (*b*) DR_F/DR_{GF} (−), L_i = 40 m; (*c*) $Tilt_F/Tilt_{GF}$ (−), L_i = 60 m; (*d*) DR_F/DR_{GF} (−), L_i = 60 m; (*e*) $Tilt_F/Tilt_{GF}$ (−), L_i = 80 m; (*f*) DR_F/DR_{GF} (−), L_i = 80 m.

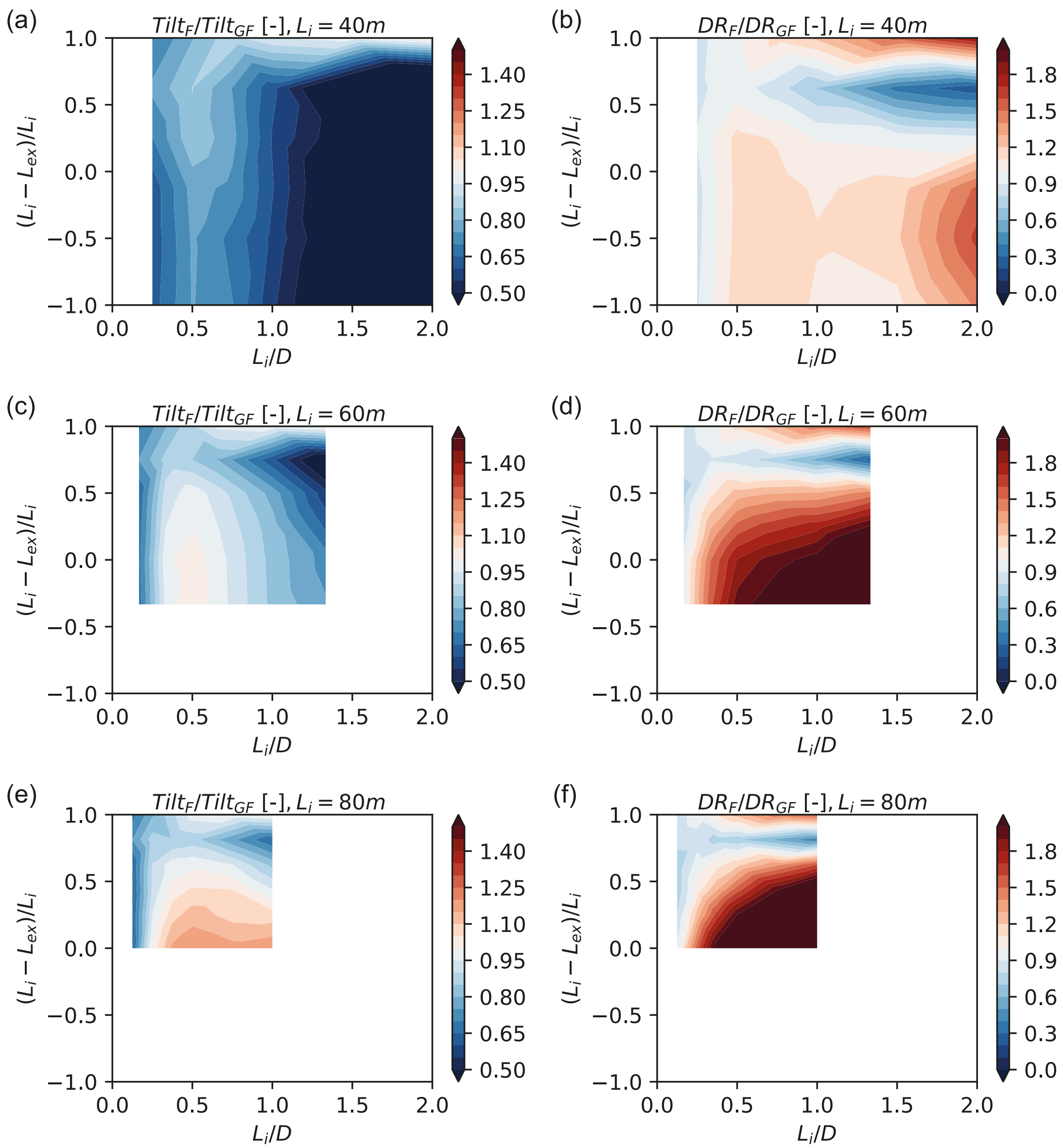

Fig. 13. Influence of geometry on pile response for piling induced displacements: (*a*) vertical relative restraint; (*b*) horizontal relative restraint; (*c*) normalised maximum axial strain; (*d*) normalised maximum deflection ratio; (*e*) normalised location of maximum axial strain; (*f*) normalised maximum curvature.

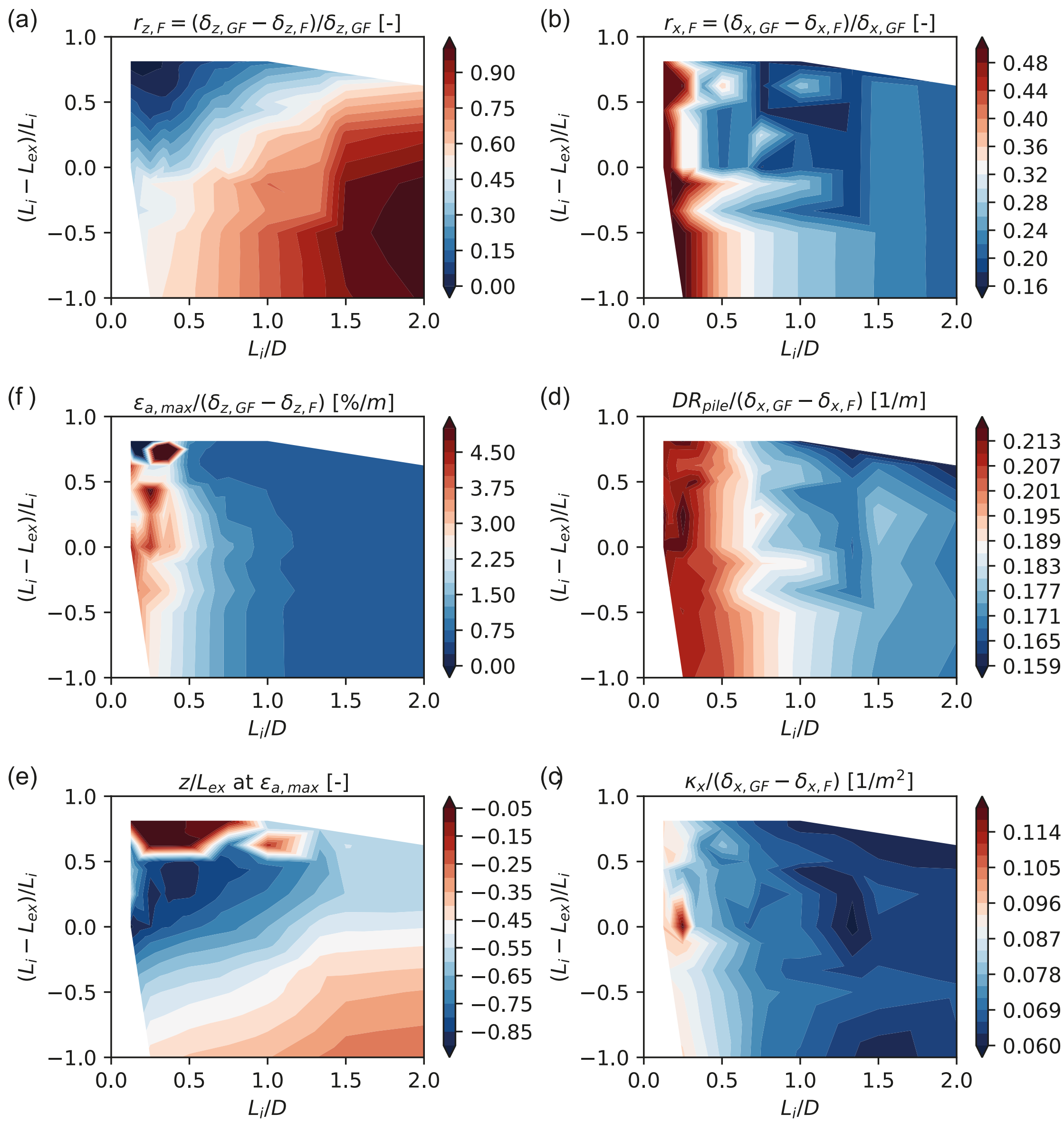

also increases with the length of the existing piles. The horizontal relative restraint $r_{x,F}$, see Fig. 13*b*, is below 1, indicating that the pile is held back compared to the GF displacement. $r_{z,F}$ decreases with the increased distance from the installed pile. Figure 13*c* shows that the axial strain ε_a in the pile normalised with the restrained vertical displacement $\delta_{z,GF} - \delta_{z,F}$ is decreasing with an increasing distance from the installed pile. The location of the $\varepsilon_{a,max}$ normalised with L_{ex} is presented in Fig. 13*e*. These maximum values is located in the bottom 2/3 of the pile for all intermediate configurations, while the location is near the top of the pile for relatively long and short existing piles. The DR_{pile} of the front pile is normalised with the horizontal displacement difference $\delta_{x,GF} - \delta_{x,F}$, to study the effect in relation to the restraint (i.e., independent of the decreasing displacements with increasing distance from the foundation) (see Fig. 13*d*). The ratio ranges between 0.16 and 0.21 and decreases with the increased distance from the installed pile. The curvature κ_x of the front pile is, similar to DR_{pile}, normalised with the horizontal displacement difference $\delta_{x,GF} - \delta_{x,F}$ and ranges between 0.06 and 0.11. Smaller values are found at an increased distance from the installed pile group, (see Fig. 13*f*).

4.2. Foundation stiffness

The second part of the sensitivity study focuses on the influence of the number of piles, the pile stiffness, the slab stiffness and the size of the existing foundation. The range of the stiffness parameters studied are summarised in Table 8, and the foundation geometry and the pile spacing are presented in Table 9. The ratio between the stiffness in the soil at the

Table 8. Parameter range for the influence study on foundation stiffness.

E_{pile} (MPa)	E_{soil} (MPa)	E_{slab} (MPa)
(8.63–6) × 10^5	2.8–56.25	(0.3–6) × 10^6

Table 9. Parameter range for the influence study on foundation geometry.

ctc_x (m)	ctc_y (m)	b (m)	w (m)
1.5–18	1.5–18	9–27	10.5–31.5

surface and the stiffness increment towards depth are kept constant for the parametric study. Although not representative of any practical stiffness of an existing foundation, the cases where the stiffness of either the pile or the slab is substantially lower than the soil stiffness are included. The latter, respectively, represent the limiting cases of a slab without piles and a pile group without a slab.

The parametric study shows that the response of the system is identical when the relative stiffness between the soil and the pile E_{soil}/E_{pile} and between the soil and the slab E_{soil}/E_{slab} are kept constant, which is in line with other geotechnical SSI problems (e.g., Muir Wood 2004). The influence of the stiffness and geometry of the foundation on the response of the foundation slab is shown in Fig. 14. In this figure the relative stiffness between the pile and the soil E_{soil}/E_{pile}, the relative stiffness between the soil and the slab E_{soil}/E_{slab}, the centre-to-centre distance of the piles in both directions ctc_x and ctc_y are varied, while keeping the dimensions of the foundation constant at $b = 18$ m, $w = 21$ m. In addition, the impact of an increased surface area for the foundation is investigated, whilst keeping the ctc_x and ctc_y to 3 m. The parameterised study generally indicates a limited effect from the mean relative horizontal restraint. The mean relative vertical restraint is strongly influenced by the stiffness ratio E_{soil}/E_{pile}, as shown in Fig. 14*a*. The influence of pile stiffness, however, is secondary to the main effects of the relative distance and the pile length, as highlighted in Fig. 13*a*.

The tilt and deflection ratios are largest for intermediate stiffness ratios. The relative stiffness between the soil and the slab, see Fig. 14*b*, has a limited influence on the mean relative vertical and horizontal restraint, while showing a strong influence on the tilt and deflection ratio of the slab. Increasing the number of piles impacts all response parameters for the slab, except the horizontal restraint (Fig. 14*c*). A decrease in individual pile efficiency with an increasing number of piles is observed, i.e., the vertical restraint increases linearly with a tenfold increase in the number of piles. The increase in foundation size strongly influences the $r_{z,F}$, whereas the other parameters are only moderately influenced (Fig. 14*d*).

The influence of the relative stiffness between the pile and the soil E_{soil}/E_{pile} and the relative stiffness between the soil and the slab E_{soil}/E_{slab} on the response of the front pile in the existing pile group are presented in Figs. 15*a* and 15*b*. The vertical restraint is strongly linked to the relative pile stiffness, whereas the influence of the slab stiffness is limited. In contrast, the horizontal restraint shows the opposite response, where a strong influence is found for the relative soil and slab stiffness. Furthermore, the horizontal restraint is not much affected by the relative soil and pile stiffness. Thus, the influence on the horizontal displacement field from the pile installation can almost completely be attributed to the presence of an existing shallow slab, whereas the influence on vertical displacement is strongly linked to the stiffness of the piles below the slab.

The influence of the number of piles in the existing pile group, whilst keeping the foundation area constant ($b = 18$ m, $w = 21$ m), is plotted in Fig. 16*b*. The results indicate an increase in vertical restraint with an increased number of piles. Simultaneously, the efficiency of each pile decreases with additional piles. κ_x and ε_a also decrease, indicating a lower force acting in each pile. Figure 16*a* shows the influence of changing the foundation area while keeping ctc_x and ctc_y constant at 3 m. The results show that the increase of foundation area is increasing the vertical restraint. A similar trend is also shown in Fig. 14*d*. Furthermore, the horizontal restraint of the existing structure is strongly affected by the size of the foundation. The difference between the mean displacement of the slab and the displacement at the location of the front pile increases as a function of the size of the foundation.

The data in Figs. 14, 15, and 16 can be combined with the modification factors for the problem geometry, i.e., Fig. 13, to include deviations in foundation properties from the reference case.

5. Application of the non-dimensional results

The use of the non-dimensional charts to predict the deformations of the first pile in an existing pile group due to nearby piling is elaborated in the following example. For simplicity, the same properties are used for the existing pile, slab and soil as the case presented in Fig. 9.

A group of 50 displacement piles with a length L_i of 40 m and a cross-sectional area of 0.1 m^2 are installed adjacent to an existing structure on a deep foundation. The existing foundation has a spacing between the 40 m long piles of 3 m with a foundation area of 20×20 m^2. The soft clay deposit has a consolidation coefficient $c_v = 5 \times 10^{-7}$ $m^2 s^{-1}$ and the piles are installed at a rate > 10 mh^{-1}. The corresponding normalised penetration velocity becomes ≈2000, which is larger than the limit value for an undrained system response of 20. The centre of mass of the new pile group is located 20 m from the closest edge of the existing building. For simplicity, the 50 displacement piles are grouped into one pile located in the centre.

The displacements are estimated from Fig. 7*a* with the total area of the piles $\Omega = 50 \cdot 0.1 = 5$ m^2. The average movement of the existing foundation is based on the average GF movement from the front and back end of the slab. The front end is located at a normalised position of $r/L_i = 20/40 = 0.5$, which gives a $\delta_r = \frac{1.05 \cdot 5\ m^2}{40\ m\pi} = 4.2$ cm, and a $\delta_z = \frac{0.44 \cdot 5\ m^2}{40\ m\pi} = 1.7$ cm.

Fig. 14. Influence study on the slab response due to piling-induced displacements. The cross indicates the results from the reference configuration as illustrated in Section 3.3: (*a*) relative stiffness between soil and pile; (*b*) relative stiffness between soil and slab; (*c*) number of piles; (*d*) foundation size.

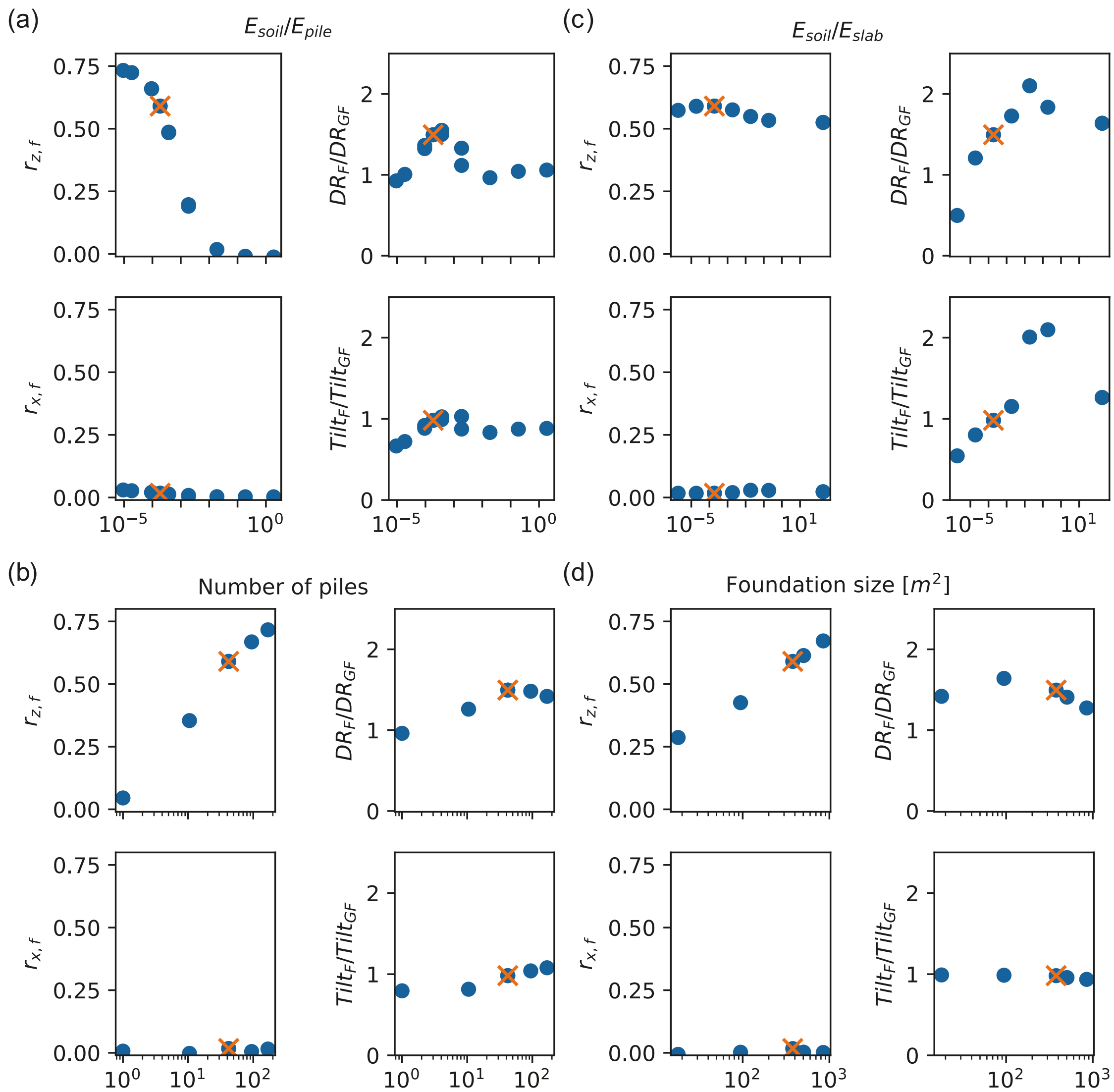

The back end is located at a normalised position of $r/L_i = 20/40 = 1$, which gives a $\delta_r = \frac{0.43 \cdot 5\ \mathrm{m}^2}{40\ \mathrm{m}\pi} = 1.7\,\mathrm{cm}$, and a $\delta_z = \frac{0.14 \cdot 5\ \mathrm{m}^2}{40\ \mathrm{m}\pi} = 0.6\,\mathrm{cm}$.

The restraint in the horizontal direction of the front pile is calculated as the difference from the mean movement of the slab to $4.2\,\mathrm{cm} - \frac{4.2\,\mathrm{cm}+1.7\,\mathrm{cm}}{2} = 1.25\,\mathrm{cm}$. Figure 13*a* with $(L_i - L_{ex})/L_i = 0$ and $L_i/D = 0.5$ gives a relative vertical restraint of 0.6, which result in a vertical movement of $0.6 \cdot 1.8\,\mathrm{cm} - 1.8\,\mathrm{cm} = -0.72\,\mathrm{cm}$. Following from the restrained horizontal movement in the top of the pile head, the curvature of the existing pile is estimated from Fig. 13*f* to $0.08 \cdot 1.25\,\mathrm{cm} = 0.001\,\mathrm{m}^{-1}$. The axial strain is estimated from Fig. 13*c* combined with the restrained vertical movement to $2.5\,\%\,\mathrm{m}^{-1} \cdot -0.72\,\mathrm{cm} = 0.018\%$. The moment is calculated as $M = \kappa \mathrm{EI} = 0.001 \cdot 30\,\mathrm{GPa} \cdot 4.78 \times 10^{-4}\,\mathrm{m}^{-4} = 14.3\,\mathrm{kNm}$. The maximum axial tensile force are calculated by the formula $F = A\varepsilon E = 0.076\ \mathrm{m}^2 \cdot 0.00018 \cdot 30\,\mathrm{GPa} = 567\,\mathrm{kN}$ and is located at a depth of about $0.75 \cdot L_i = 30\,\mathrm{m}$ following Fig. 13*e*.

6. Conclusions

The impact of nearby piling on existing piled structures has been investigated with the focus on finding modification factors to incorporate SSI into predicted (or measured) displacement fields in GF conditions. A simplified parameterised three-dimensional FE model was created to systematically study the effect of various newly proposed (dimensionless) factors of the new and existing pile group and their impact on the displacement field and structural response.

The results show that the distribution of soil displacements is altered due to the presence of an existing structure, compared to a GF situation, thus highlighting the need to account for SSI when analysing the response of existing structures. In general, an existing foundation slab is shown to be displaced with a uniform horizontal displacement equal to the mean GF displacements at the location of the slab. Pinned

Fig. 15. Influence study on the pile response due to piling-induced displacements. The cross indicates the results from the reference configuration as illustrated in Section 3.3: (*a*) relative stiffness between soil and pile; (*b*) relative stiffness between soil and slab.

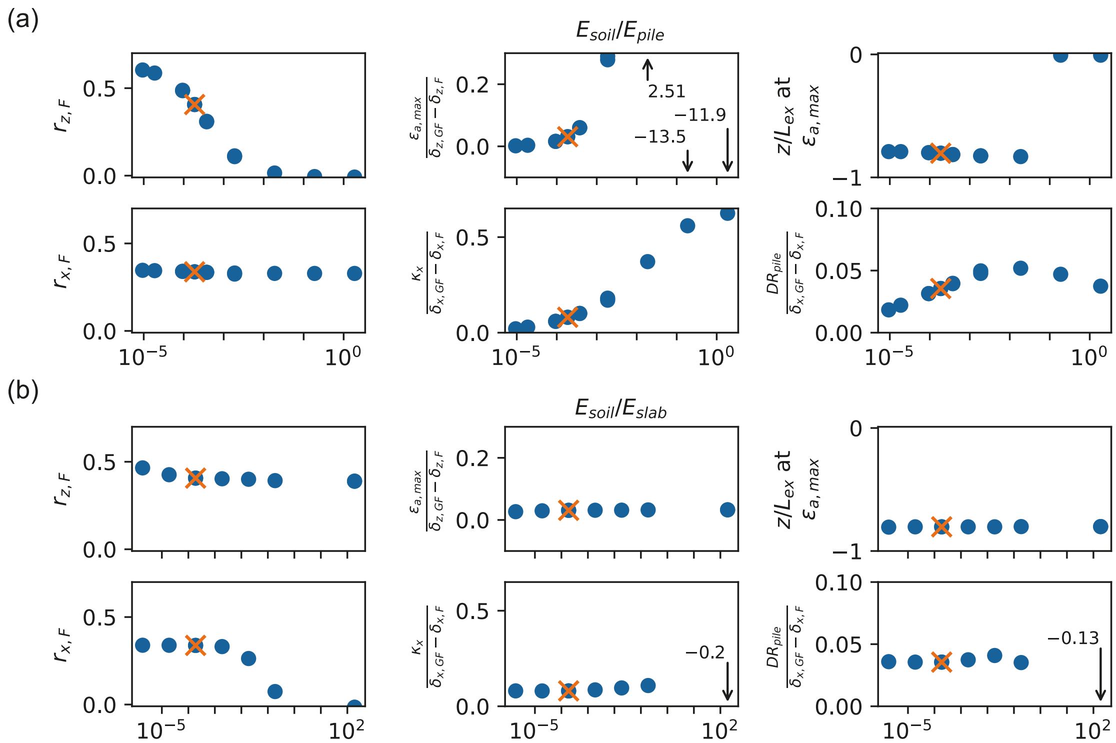

Fig. 16. Influence study on the pile response due to piling-induced displacements. The cross indicates the results from the reference configuration as illustrated in Section 3.3: (*a*) influence of foundation size for a constant ctc between piles of 3 m; (*b*) influence of number of piles for a foundation with constant size of 18 × 21 m^2.

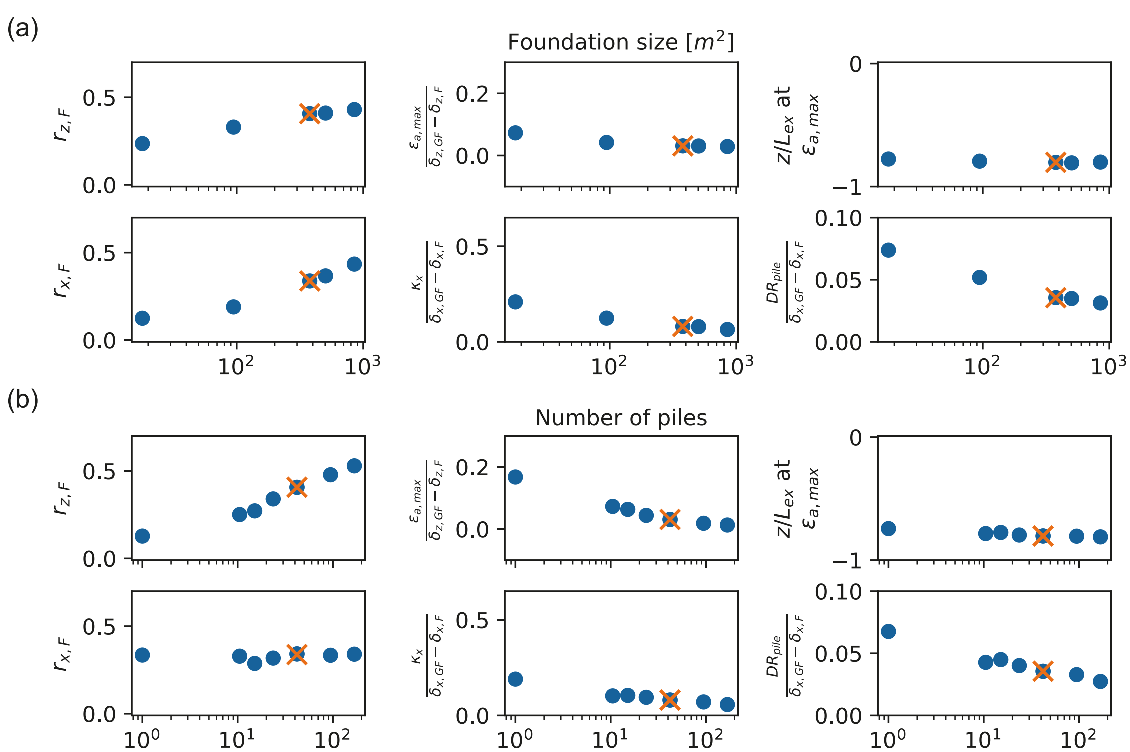

pile heads follow the slab, whereas the lower part of the pile follows the movement of the surrounding soil, which leads to large horizontal deformations in the upper part of the pile.

A parametric study was conducted as a first step towards finding a set of generalised modification factors relating the GF movement to the response of an existing piled structure. Restraint factors that normalise the difference between displacements in GF conditions and the response with an existing structure have been proposed. These restraint factors can be uniquely linked to the ratio of the newly installed pile length L_i and distance D between the new and existing pile group L_i/D and the normalised difference in length between the newly installed and existing pile L_{ex}, i.e., $(L_i - L_{\mathrm{ex}})/L_i$ (Fig. 13).

The parametric study further shows that:

- Existing piles restrain the vertical displacements of existing foundations. In contrast, the impact of the pile on the horizontal displacement of the existing structure is limited.
- A foundation slab restrains horizontal displacements without substantially influencing the vertical displacements.
- The deflection ratio and curvature of existing piles is strongly linked to the horizontal restraint of the pile head.
- The mean relative vertical restraint of the foundation slab is strongly influenced by the foundation size and spacing of piles while the influence on the slabs relative horizontal restraint is limited.

In addition to the influence of the existing foundation, the depth and horizontal extent of the soil deposit were found to influence the magnitude of the GF displacements from pile installation. The non-dimensional response proposed by Sagaseta and Whittle (2001) should be modified to consider the size of the considered domain in situations where the assumption of pile installation into an infinite half-space is not applicable.

In conclusion, the charts that summarise the results of this study are considered as a starting point for relating the GF displacements to the response of existing piled structures, using modification factors. The modification factor approach is not intended to fully replace a detailed case specific analysis, rather they are intended to aid the early design process, as well as give asset owners the tools to evaluate the impact of piling works.

Acknowledgements

The first author acknowledges the financial support provided by SBUF (Development fund of the Swedish construction industry, grants 13614 and 14186), BIG (Better Interaction in Geotechnics), grants A2019-19 and B2019-19, from the Swedish Transport Administration and NCC AB. The work is done as part of Digital Twin Cities Centre that is supported by Sweden's Innovation Agency VINNOVA under Grant No. 2019-00041.

Article information

History dates

Received: 12 July 2024
Accepted: 8 January 2025
Accepted manuscript online: 13 January 2025
Version of record online: 13 March 2025

Copyright

Data availability

Data are available upon request.

Author information

Author ORCIDs

Jonatan Isaksson https://orcid.org/0000-0003-1863-1508
Jelke Dijkstra https://orcid.org/0000-0003-3792-0727

Author contributions

Conceptualization: JI, MK, JD
Data curation: JI
Formal analysis: JI
Funding acquisition: JD
Investigation: JI
Methodology: JI, MK, JD
Project administration: JD
Resources: MK, JD
Supervision: MK, JD
Validation: JI
Visualization: JI
Writing – original draft: JI, JD
Writing – review & editing: JI, JD

Competing interests

The authors declare there are no competing interests.

References

Abu-Farsakh, M., Rosti, F., and Souri, A. 2015. Evaluating pile installation and subsequent thixotropic and consolidation effects on setup by numerical simulation for full-scale pile load tests. Canadian Geotechnical Journal, **52**(11): 1173–1746. doi:10.1139/cgj-2014-0470.

Basmaji, B., Deck, O., and Al Heib, M. 2019. Analytical model to predict building deffiections induced by ground movements. European Journal of Environmental and Civil Engineering, **3**: 409–431. doi:10.1080/19648189.2017.1282382.

Bozozuk, M., Fellenius, B.H., and Samson, L. 1978. Soil disturbance from pile driving in sensitive clay. Canadian Geotechnical Journal, **15**(3): 346–361. doi:10.1139/t79-048.

Brinkgreve, R., Kumarswamy, S., Swolf, W., Fonseca, F., Ragi Manoj, N., Zampich, L., and Zalamea, N. 2023. PLAXIS 3D, 2023.2. Plaxis bv, Bentley Systems, Incorporated, Netherlands.

Burland, J. 1997. Assesment of risk of damage to buildings due to tunneling and excavation. Earthquake Geotechnical Engineering, Balkema, Rotterdam, The Netherlands. pp. 1189–1201.

Dao, T. 2011. Validation of PLAXIS embedded piles for lateral loading. M.Sc. thesis, Faculty of Civil Engineering and Geosciences, Delft University of Technology, Delft, Netherlands.
Deck, O., and Singh, A. 2012. Analytical model for the prediction of building deflections induced by ground movements. International Journal for Numerical and Analytical Methods in Geomechanics, **36**: 62–84. doi:10.1002/nag.993.
Dias, T., and Bezuijen, A. 2015. Data analysis of pile tunnel interaction. Journal of Geotechnical and Geoenvironmental Engineering, **141**(28): 04015051. doi:10.1061/(ASCE)GT.1943- 5606.0001350.
Dugan, J.P., Jr., and Freed, D.L. 1984. Ground heave due to pile driving. *In* 1st International Conference on Case Histories in Geotechnical Engineering. St. Louis, Missouri. Available from https://scholarsmine.mst.edu/icchge/1icchge/1icchge-theme1/28.
Edstam, T., and Kullingsjö, A. 2010. Ground displacements due to pile driving in Gothenburg clay. *In* NUMGE 2010 : 7th European Conference on Numerical Methods in Geotechnical Engineering. *Edited by* Benz and Nordal. Taylor & Francis Group, London. pp. 625–630.
Franza, A., Deck, O., and DeJong, M. 2020. Charts for the mining-induced deflection of buildings. Canadian Geotechnical Journal, **57**: 2020–2026. doi:10.1139/t79-048.
Franza, A., Marshall, A.M., Haji, T., Abdelatif, A.O., Carbonari, S., and Morici, M. 2017. A simplified elastic analysis of tunnel-piled structure interaction. Tunnelling and Underground Space Technology, **61**: 104–121. doi:10.1016/j.tust.2016.09.008.
Franza, A., Zheng, C., Marshall, A., and Jimenez, R. 2021. Investigation of soil–pile–structure interaction induced by vertical loads and tunnelling. Computers and Geotechnics, **139**: 104386. doi:10.1016/j.compgeo.2021.104386.
Franzius, J.N., Potts, D.M., and Burland, J.B. 2006. The response of surface structures to tunnel construction. Proceedings of the Institution of Civil Engineers - Geotechnical Engineering, **159**(1): 3–17. doi:10.1680/geng.2006.159.1.3.
Goh, K.H., and Mair, J.M. 2014. Response of framed buildings to excavation-induced movements. Soils and Foundations, **54**(3): 250–268. doi:10.1016/j.sandf.2014.04.002.
Hagerty, D., and Peck, R. 1971. Heave and lateral movements due to pile driving. Proceedings of the American Society of Civil Engineers, **97**(11): 1513–1532. doi:10.1061/JSFEAQ.000170.
Hunt, E.H., Pestana, J.M., Bray, J.D., and Reimer, M. 2002. Effect of pile driving on static and dynamic properties of soft clay. Journal of Geotechnical and Geoenvironmental Engineering, **128**(1): 13–24. doi:10.1061/(ASCE)1090-0241(2002)128:1(13).
Isaksson, J. 2022. A numerical study on massdisplacements from piling in natural clay. Technical report for mid-term seminar, Department of Architecture and Civil Engineering, Chalmers University of Technology, Göteborg, Sweden. Available from https://www.sbuf.se/Projektsida?project=f3dad4d5-565e-4a27-9904-d08b5e918204.
Karlsrud, K., and Haugen, T. 1985. Axial static capacity of steel model piles in over- consolidated clay. In Proc. 11th Int. Conf. Soil Mech. Found. Eng. Vol. 3. pp. 1401–1406.
Korff, M. 2012. Response of piled buildings to the construction of deep excavations. PhD thesis, Department of Engineering, University of Cambridge, Cambridge, UK.
Lehane, B., and Gill, D. 2004. Displacement fields induced by penetrometer installation in an artificial soil. International Journal of Physical Modelling in Geotechnics, **1**: 25–36. doi:10.1680/ijpmg.2004.040103.
Lehane, B., and Jardine, R. 1994. Displacement-pile behaviour in a soft marine clay. Canadian Geotechnical Journal, **31**(2): 181–191. doi:10.1139/t94-024.
Lehane, B.M., O'loughlin, C.D., Gaudin, C., and Randolph, M.F. 2009. Rate effects on penetrometer resistance in kaolin. Geotechnique, **59**(1): 41–52. doi:10.1680/geot.2007.00072.
Mair, R.J. 2013. Tunnelling and deep excavations: Ground movements and their effects. *In* Proceedings of the 15th European Conference on Soil Mechanics and Geotechnical Engineering - Geotechnics of Hard Soils – Weak Rocks (Part 4). *Edited by* A. Anagnostopoulos, M. Pachakis and T. Tsatsanifos. IOS Press, Amsterdam, Netherlands. pp. 39–70.
Monforte, L., Gens, A., Arroyo, M., Mánica, M., and Carbonell, J. 2021. Analysis of cone penetration in brittle liquefiable soils. Computers and Geotechnics, **134**: 104123. doi:10.1016/j.compgeo.2021.104123.
Muir Wood, D. 2004. Geotechnical modelling. CRC Press, London.
Ni, Q., Hird, C., and Guymer, I. 2010. Physical modelling of pile penetration in clay using transparent soil and particle image velocimetry. Géotechnique, **60**(2): 121–132. doi:10.1680/geot.8.P.052.
Pestana, J.M., Hunt, C.E., and Bray, J.D. 2002. soil deformation and excess pore pressure field around a closed-ended pile. Journal of Geotechnical and Geoenvironmental Engineering, **128**(1): 669–671. doi:10.1061/(ASCE)1090-0241(2003)129:7(669).
Potts, D.M., and Addenbrooke, T.I. 1997. A structure's influence on tunneling-induced ground movements. Proceedings of the Institution of Civil Engineers - Geotechnical Engineering, **125**(2): 109–125. doi:10.1680/igeng.1997.29233.
Poulos, H.G., and Davis, E.H. 1980. Pile foundation analysis and design. John Wiley and Sons, New York, NY.
Randolph, M.F., Carter, J.P., and Wroth, C.P. 1979. Driven piles in clay—the effects of installation and subsequent consolidation. Géotechnique, **29**(4): 361–393. doi:10.1680/geot.1979.29.4.361.
Sadek, M., and Shahrour, I. 2004. A three dimensional embedded beam element for reinforced geomaterials. International Journal for Numerical and Analytical Methods in Geomechanics, **28**: 931–946. doi:10.1002/nag.357.
Sagaseta, C., and Whittle, A. 2001. Prediction of ground movements due to pile driving in clay. Journal of Geotechnical and Geoenvironmental Engineering, **127**(1): 55–66. doi:10.1061/(ASCE)1090-0241(2001)127:1(55).
Sagaseta, C., Whittle, A., and Santagata, M. 1997. Deformation analysis of shallow penetration in clay. International Journal for Numerical and Analytical Methods in Geomechanics, **21**(10): 687–719. doi:10.1002/(SICI)1096-9853(199710)21:10⟨687::AID-NAG897⟩3.0.CO;2-3.
Sheil, B., and McCabe, B. 2012. Predictions of friction pile group response using embedded piles in PLAXIS. *In* 3rd International Conference on New Developments in Soil Mechanics and Geotechnical Engineering. Near East University, Nicosia, Cyprus.
Sheil, B., McCabe, B.A., Hunt, C.E., and Pestana, J.M. 2015. A practical approach for the consideration of single pile and pile group installation effects in clay: Numerical modelling. Journal of Geo-Engineering Sciences, **2**: 119–142. doi:10.3233/JGS-140027.
Tschuchnigg, F., and Schweiger, H. 2015. The embedded pile concept—verification of an efficient tool for modelling complex deep foundations. Computers and Geotechnics, **63**: 244–254. doi:10.1016/j.compgeo.2014.09.008.
Wang, D., Bienen, B., Nazem, M., Tian, Y., Zheng, J., and Pucker, T. M.F., R. 2015. Large deformation finite element analyses in geotechnical engineering. Computers and Geotechnics, **65**: 104–114. doi:10.1016/j.compgeo.2014.12.005.
Xu, K., and Poulos, H. 2001. 3-D elastic analysis of vertical piles subjected to "passive" loadings. Computers and Geotechnics, **28**: 349–375. doi:10.1016/S0266-352X(00)00024-0.
Zheng, C., Franza, A., and Jimenez, R. 2023. Analysis of floating and end-bearing pile foundations affected by deep-excavations. Computers and Geotechnics Journal, **153**: 105075. doi:10.1016/j.compgeo.2022.105075.
Zhou, H., Lui, H., Randolph, M., Kong, G., and Cao, Z. 2017. Experimental and analytical study of X-section cast-in-place concrete pile installation effect. International Journal of Physical Modelling in Geotechnics, **17**(2): 103–121. doi:10.1680/jphmg.15.00037.